Langmuir

Article

pubs.acs.org/Langmuir

Hysteresis Loop and Scanning Curves of Argon Adsorption in Closed-End Wedge Pores

Nikom Klomkliang,[†,‡] D. D. Do,[*,†] and D. Nicholson[†]

[†]School of Chemical Engineering, University of Queensland, St. Lucia, Queensland 4072, Australia

[‡]Chemical Engineering Program, Faculty of Engineering, Naresuan University, Phitsanulok 65000, Thailand

ABSTRACT: The hysteresis loop and scanning curves for argon adsorbed in a wedge pore with one end closed are studied with grand canonical Monte Carlo simulation. We have found multiple hysteresis loops for pores with either the narrow end or the wider end closed. In pores with the narrow end closed, adsorption and desorption exhibits a two-stage sequence of rapid change, followed by a gradual change in adsorbate density. The pore can be divided into zones of commensurate packing and junctions of incommensurate packing. A striking feature is that the sequence of these two stages is opposite for the adsorption and desorption processes. This can be explained by cohesion in the adsorbate, in which a steep condensation process is associated with the zones and a steep evaporation process is associated with the junctions between them. For pores with the wider end closed, the processes of adsorption and desorption from various zones are correlated with each other. In pores with the narrow end closed, the scanning curves trace reversibly along the segment of the isotherm, where the isotherm shows gradual change, and when the scanning curve reaches a point between the gradual change segment and the sharp change segment, the scanning curve crosses from one boundary of the hysteresis loop to the corresponding point on the other boundary. This indicates that the condensation and evaporation states are not affected by scanning but that, in scanning across the hysteresis loop, the adsorbate passes through a sequence of metastable states as the distribution of density is rearranged, without any significant change in the overall density. In contrast, for pores with the wider end closed, both the descending curve from a partially filled pore and the ascending curve are identical to the desorption branch of the corresponding pore with its narrow end closed.

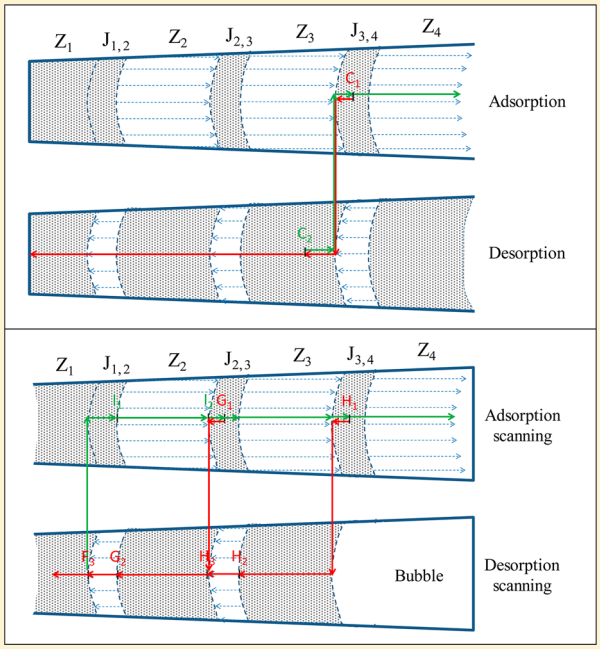

1. INTRODUCTION

In the characterization of porous solids by gas adsorption, the shape of the hysteresis loop does not provide sufficient information to draw unequivocal conclusions about the pore structure of an adsorbent.[1,2] Examination of the variation in the shape of the hysteresis loop with the temperature[3−6] provides useful extra information, but supplementary evidence is necessary. It has been suggested that a way to probe deeper into the pore structure of a solid adsorbent would be to use data from scanning curves. A recent study by Hitchcock et al.[7] combined adsorption and mercury scanning experiments on silica sol−gel spheres to show that shielded cavities in through pores are undetectable by simple experiments. In addition scanning curves, different adsorbates and measurements over a range of temperatures are useful extensions of simple isotherm measurements as an aid to the detailed characterization of the pore structure of a porous solid.[8−13]

A scanning curve is produced by reversing the adsorption/desorption process over the pressure range, where the pores are being filled or emptied by condensation or evaporation. An early theory of sorption hysteresis based on a concept of independent domains proposed by Everett and Smith[14] is able to account for a number of experimental observations and has been more recently investigated in detail using computer simulation[15,16] for assemblies of cylindrical pores. The key idea of the domain theory is that each pore space can fill and empty independent of the state of its neighbors. However, as stressed by Coasne et al.,[15] the theory does not allow for the existence of an adsorbate film prior to condensation. Monson[10] used a lattice density functional theory (DFT) to study adsorption, desorption, and scanning in pores with rectangular cross-sections and in ink-bottle structures. Cimino et al.[12] reviewed experimental scanning data for several porous materials and formulated a model based on simulations in a cubic network,

Received: September 10, 2014
Revised: October 13, 2014
Published: October 14, 2014

   dx.doi.org/10.1021/la5035992 | *Langmuir* 2014, 30, 12879−12887

which offers a practical methodology for calculating network connectivity. Scanning in networks has also been investigated by Rojas and co-workers.[13]

In arrays of connected pores with different degrees of connectivity, a number of other forms of scanning curves have been observed, for example, (i) crossing between boundaries, (ii) converging to its closure point, and (iii) returning back to the boundary.[8−10,12,13,17−19] Most theoretical studies have used parallel-sided pore models; however, this exact geometry is unlikely to be found in real materials. Here, we show, by carrying out computer simulations for an argon adsorbate at a range of temperatures in wedge-shaped pores, that domains of commensurate and incommensurate packing can significantly affect adsorption and scanning behavior.

2. SIMULATION MODEL AND METHOD

Grand canonical Monte Carlo (GCMC)[20] was used to simulate the adsorption−desorption isotherms of argon in wedge-shaped pores with a closed narrow end or closed wide end. The wedge pore model simulates a simple connectivity between pores of linearly varying width along the line of connectivity. The pore walls and the closed end were modeled as three graphene layers whose separation distance is 0.3354 nm. The axial pore length was 30 nm, and the half angle of the wedge is 1.0°. The widths of the narrow end and the wide end were 1.953 and 3 nm, respectively.

The Lennard−Jones (LJ) 12-6 potential was used to calculate the argon−argon potential energy with a collision diameter (σ_{ff}) of 0.3405 nm and energy well depth (ε_{ff}/k_B) of 119.8 K. The interaction between argon and the pore walls was calculated from the Bojan−Steele equation[21−23] by assuming that the lengths in the y and z directions are finite and the length in the x direction (perpendicular to the page) is infinite. The number of trial moves in the GCMC simulation was at least 8×10^8 configurations, of which the first 4×10^8 configurations were used for equilibration and the remainder were used for computing the ensemble averages. Three types of trial moves: displacement, insertion, and deletion were attempted with equal probability at each simulation step. The outputs from a simulation are the average absolute volumetric densities, defined by

$$\rho_{\text{pore}}^{\text{ABS}} = \frac{\langle N \rangle}{V_{\text{acc}}} \tag{1}$$

where $\langle N \rangle$ is the ensemble average of the number of particles in the pore.

3. RESULTS AND DISCUSSION

3.1. Wedge Pore with Narrow End Closed. Before discussing the behavior of scanning curves, it is important that we establish the mechanisms of adsorption and desorption. The adsorption−desorption isotherms for argon at 70 K are shown in Figure 1. The adsorption temperature of 70 K was chosen to ensure that the hysteresis loop is wide enough to discuss the mechanism of scanning curves. The isotherms at higher temperatures show essentially the same behavior, with the exception that the width of the hysteresis loops are smaller, as will be discussed later.

Our first observation from Figure 1 is that the isotherm shows multiple hysteresis loops, whose shape is a mixture of type H1 in the International Union of Pure and Applied Chemistry (IUPAC) classification and type C (typical of a wedge pore[1,24]) in the de Boer classification. These loops are associated with distinctly different zones along the direction of the pore axis, which can be identified in the snapshot shown in Figure 2 for a completely filled pore. In the zones labeled Z_1−Z_4, there is commensurate packing of the adsorbate. These regions are separated by smaller junction regions, where the

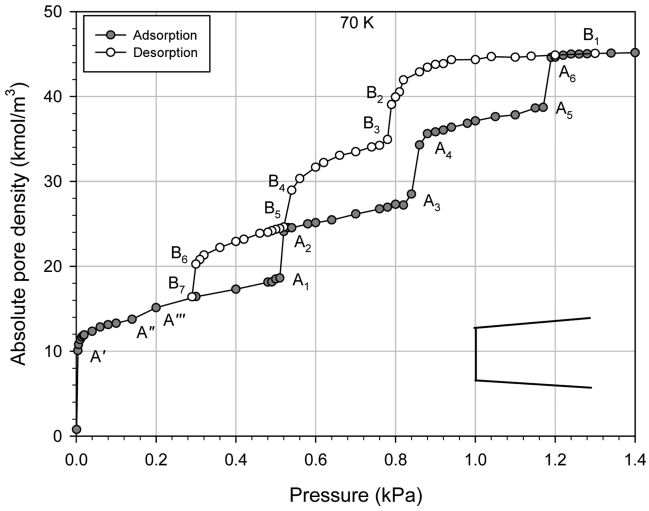

Figure 1. Adsorption−desorption isotherm of argon at 70 K in the wedge pore with the narrow end closed.

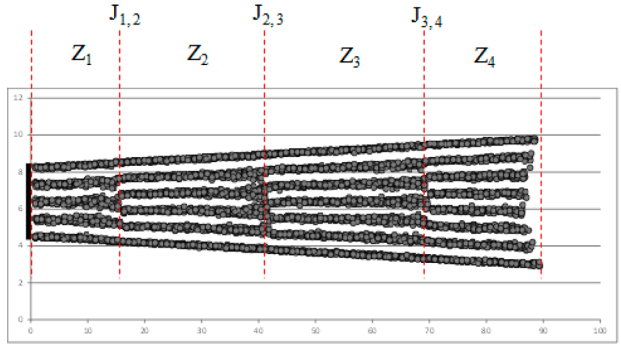

Figure 2. Illustration of the zones and junctions for adsorption in the wedge pore with the narrow end closed.

packing is incommensurate. In these junctions, we note the frustration of the adsorbate, which results in a bifurcation of the layers in the central part of the pore to form one additional layer in the next zone. We shall denote zone 1 as Z_1, the junction between zones 1 and 2 as $J_{1,2}$, etc.

Upon adsorption, adsorbate forms layers on the pore walls and at the closed end. As the pressure is increased, an interface is formed at the closed end and adsorption is favored at this curved interface because of the greater number of neighboring molecules at shorter distances than at the flat interfaces along the pore walls (Points A′−A‴ in Figure 1).

Figure 3a shows the snapshots for point A_1 just before the first condensation, where zone 1 is filled with molecules in commensurate packing and the junction $J_{1,2}$ is filled with molecules in frustrated packing. As the pressure is increased infinitesimally, there is a sharp condensation from A_1 to A_2, resulting from the sharp filling of zone 2. Beyond point A_2, there is a gradual increase in the density to point A_3, which is due to the meniscus advancing in the junction between zones 2 and 3. This process is repeated with sharp condensation in the zones (except the first zone) and gradual filling in the junctions. These successive processes are summarized in Figure 3a. The processes of sharp and gradual change in density in the zone and junction, respectively, during adsorption are opposite those occurring upon desorption, an interesting feature that will be discussed next.

dx.doi.org/10.1021/la5035992 | Langmuir 2014, 30, 12879−12887

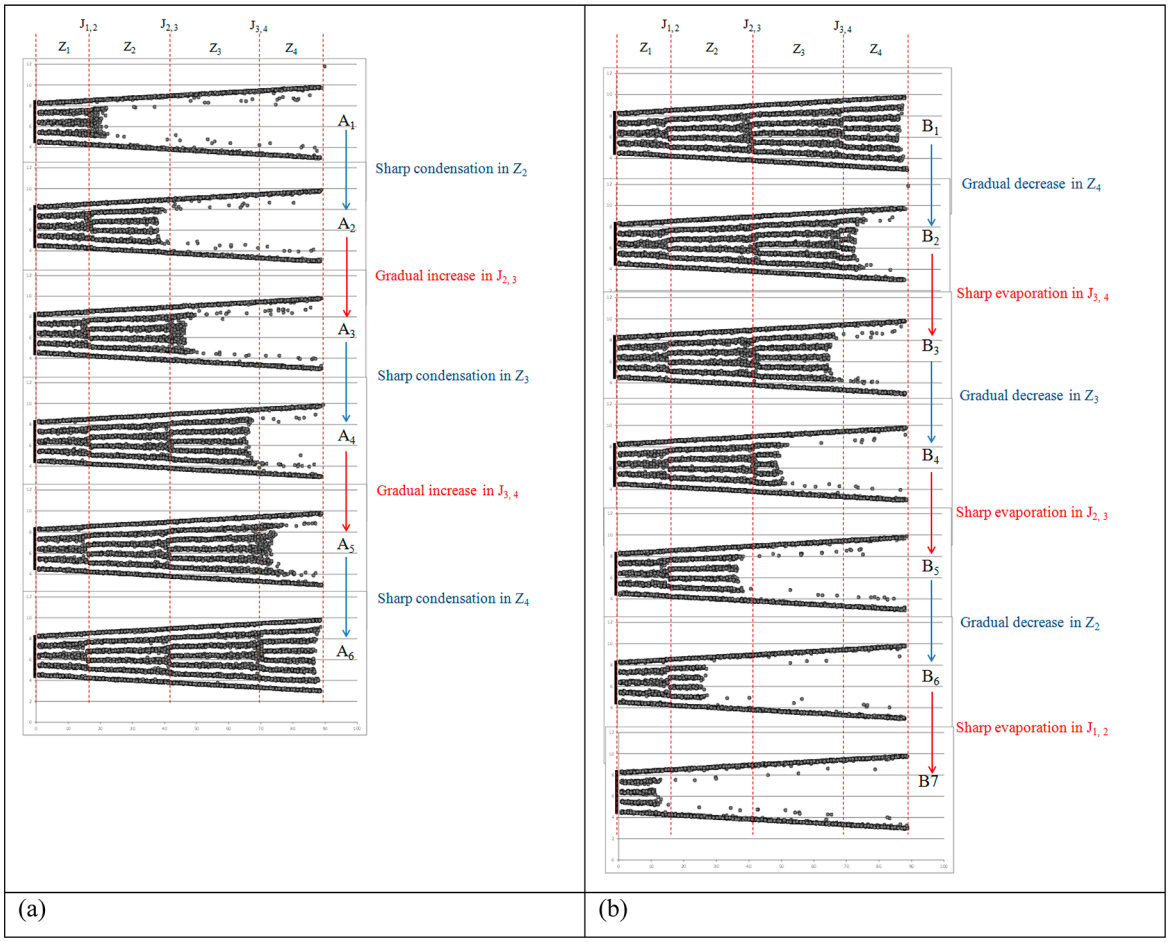

Figure 3. Snapshots of argon adsorption in the wedge pore with the narrow end closed: (a) adsorption and (b) desorption. Points A_1−A_6 and B_1−B_7 are marked on the isotherm in Figure 1.

Upon desorption from a filled pore, an interface meniscus is formed at the pore mouth, and as the pressure is decreased, the meniscus recedes in zone Z_4 to point B_2, where zone 4 has been emptied (but leaving, of course, the first layer on the pore wall). This is reflected in the gradual decrease in adsorbate density, typical of a type C hysteresis loop (de Boer classification) observed for a wedge pore and reported in our earlier work.[1,24] When point B_2 has been reached, there is a sharp evaporation from junction $J_{3,4}$. Thus, the opposite behavior from adsorption is observed in desorption; namely, (1) the sharp condensation in zones along the adsorption boundary becomes a gradual change along the desorption boundary, and (2) gradual filling in the junctions in adsorption becomes a sharp evaporation along the desorption boundary. This pattern is repeated as pressure is further decreased and summarized by the snapshots shown in Figure 3.

An important feature that emerges from this study is that the zones (where there is commensurate packing) could be viewed as being subpores connected together via junctions (this is the simplest form of connectivity where only two pores meet at a junction), and the mechanisms of adsorption and desorption occur in a sequential manner (i.e., zone−junction−zone−, etc.). This is not the case when the wider end of the pore is closed, as shown below.

Scanning Curves. We now describe the descending and ascending scanning curves within the hysteresis loop for argon adsorption at 70 K. Before getting into details, we show in Figure 4a the schematics of adsorption and desorption for ease of subsequent discussion. The regions where the gradual change in density occurs are shaded in gray, while those where sharp change occurs are represented by arrows (forward arrows for condensation and backward arrows for evaporation).

The scanning curves (descending and ascending) are shown in panels a and b of Figure 5. Obviously, the start of scanning is only possible with pressure points on the parts of the adsorption boundary or the desorption boundary with a gradual slope.

To illustrate the processes for descending scanning, we take point C_1 on the adsorption boundary as the starting point, as marked in Figures 4a and 5a, where zone 3 has been completely filled and junction $J_{3,4}$ has been partially filled. The descending scanning curve traces the adsorption boundary of the isotherm across the junction where the density change is gradual (see the red arrow in the top panel in Figure 4a). Once the adsorbate in this junction has been removed, the system then leaves the adsorption boundary, traces across the hysteresis loop, and joins the desorption boundary at the same density (see the vertical red arrow joining the two panels in Figure 4a). Upon further decrease in pressure, the system follows the desorption boundary. Therefore, what is the mechanism of spanning across the hysteresis loop? When the descending curve from point C_1 has reached the point where junction $J_{3,4}$ is emptied, it leaves the adsorption boundary and crosses the desorption boundary as junction $J_{3,4}$ is emptied. Here, the system rearranges itself as

dx.doi.org/10.1021/la5035992 | *Langmuir* 2014, 30, 12879−12887

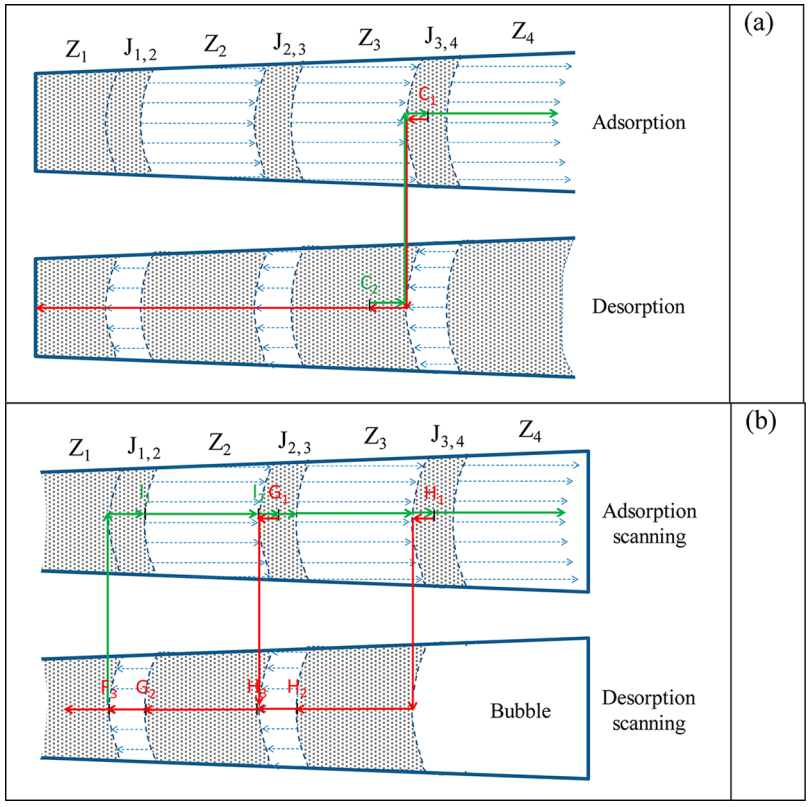

Figure 4. Schematics of adsorption and desorption in a wedge pore with the (a) narrow end closed and (b) wide end closed.

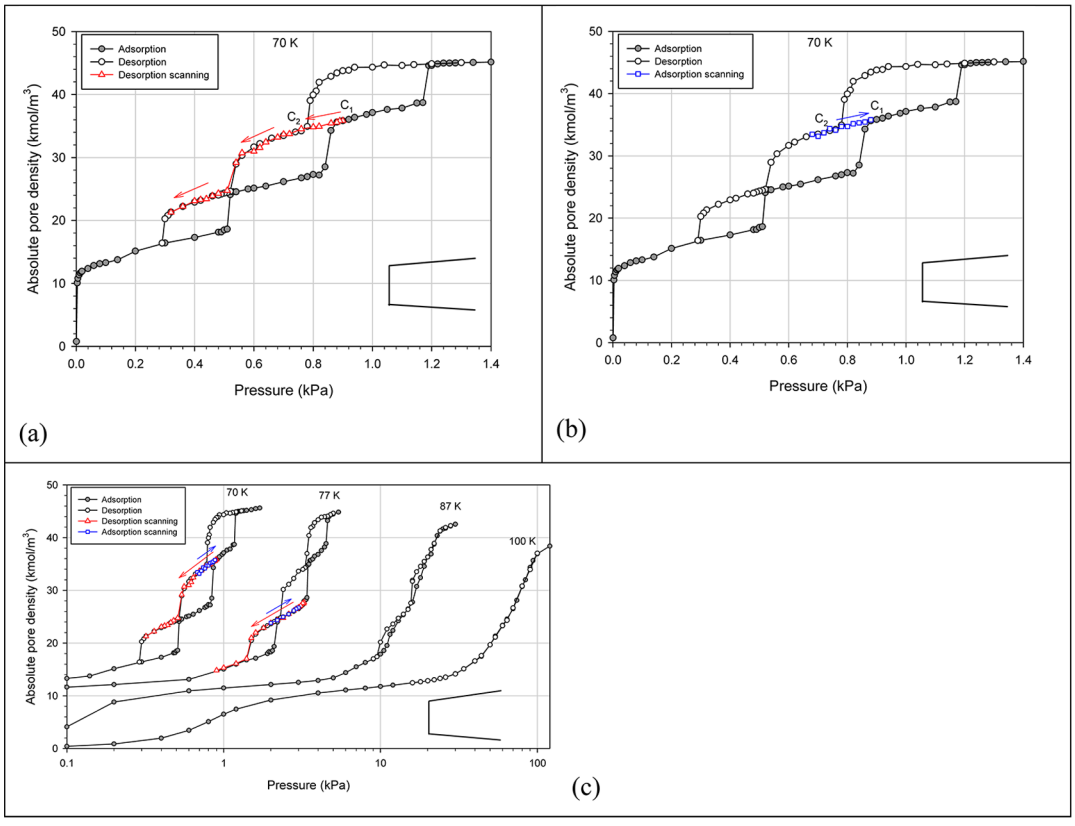

Figure 5. Primary scanning curves for argon in a wedge pore with the narrow end closed: (a) desorption scanning curve at 70 K, (b) adsorption scanning curve at 70 K, and (c) scanning curves at different temperatures.

dx.doi.org/10.1021/la5035992 | *Langmuir* 2014, 30, 12879−12887

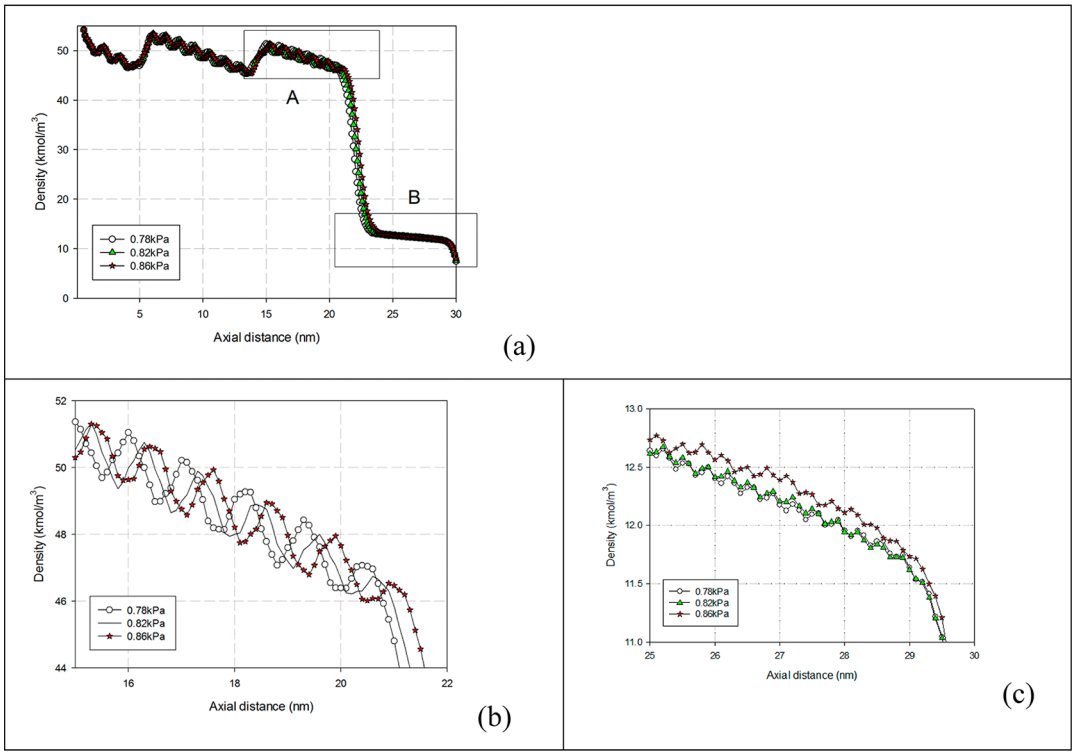

Figure 6. Density distribution along the axial direction of the pore in scanning across the loop from point C_2 to point C_1: (a) full density distribution, (b) enlargement of region A, and (c) enlargement of region B.

the pressure is decreased, at nearly a constant overall density, to evolve continuously through an uncountable number of metastable states with different density distributions along the axial direction of the pore. The axial density distributions for three states across the hysteresis loop are shown in Figure 6: two states on the adsorption and desorption boundaries and one in the middle of the hysteresis loop.

The density distributions show the four zones and the three junctions. Panels b and c of Figure 6 are enlargements of regions A and B, respectively, and illustrate the evolution of the density profile. Thus, as the system scans across the loop, it passes through a sequence of rearrangements of the molecules in the regions where the adsorbate is dense (for example, region A), while the total density remains the same. In region B, there is a small increase in the density (which is zone 4). This occurs because, as pressure is increased in scanning from the desorption boundary to the adsorption boundary, there is a buildup in the adsorbed layer in this zone. For this reason, the overall density is increased slightly from point C_2 to point C_1. The significance of the adsorbed layer in modifying the original domain theory by Everett and Smith was first noted by Coasne et al.[15]

To examine ascending scanning, we take point C_2 (where zone 3 is partially filled) on the desorption boundary of the isotherm as the starting point. When the pressure is increased, the ascending curve traces the desorption boundary until zone 3 is filled (see the horizontal green arrow in the bottom panel of Figure 4a). Once this has been achieved, the system leaves the desorption boundary, spans across the hysteresis loop, and joins the adsorption boundary in the same density as it left the desorption boundary. After that, the system follows the adsorption boundary as pressure is further increased. It is also worth noting that the process of scanning across the hysteresis loop is reversible; i.e., the descending scanning curve from C_1 is the same as the ascending curve from C_2.

The common denominator between ascending or descending scanning is that, when we start from any point along a boundary, the system traces along the path where the density change is gradual until it has reached the point where a sharp change in density begins; the scanning curve then leaves the boundary curve, crosses the hysteresis loop by rearranging the density distribution at a constant overall density, and joins the other boundary in the same state. This means that scanning across the hysteresis loop is not associated with any condensation or evaporation processes.

The effects of the temperature on the scanning curves are shown in Figure 5c. Similar scanning behavior to that discussed above for adsorption at 70 K is also observed in the other isotherms. The only difference is that the distinct loops in the 70 K isotherm become a smaller fused loop at higher temperatures, and the isotherm eventually becomes reversible when the temperature is high enough (greater than 100 K).

3.2. Wedge Pore with the Wide End Closed. The adsorption and desorption isotherms for argon adsorption at 77 K in a wedge pore with its wide end closed are shown in Figure 7. The isotherm has a hysteresis loop with type H2 characteristics, with the only difference being that the adsorption branch shows multiple condensation steps and that the desorption branch has a very large evaporation step with a small tail. The multiple condensation steps are characteristic of the low-temperature adsorption observed earlier for the pore with the narrow end closed.

The difference between the pore with the wide end closed and the pore with its narrow end closed is that desorption from a completely filled pore is not the same as desorption from a partially filled pore (i.e., the descending scanning curve), although desorption from a partially filled pore with the wide

dx.doi.org/10.1021/la5035992 | Langmuir 2014, 30, 12879−12887

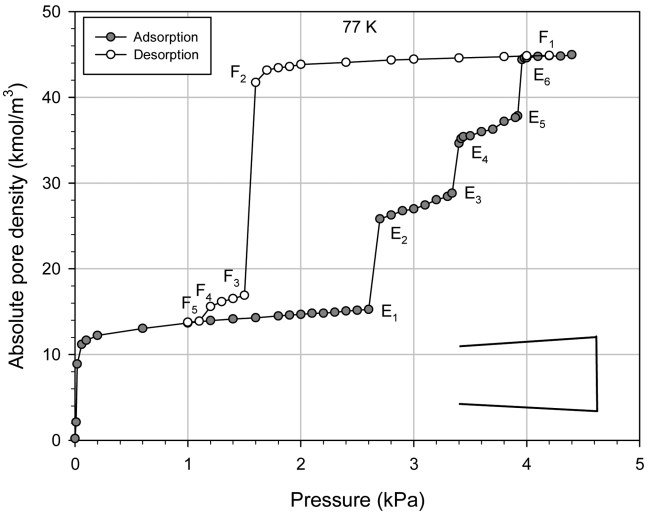

Figure 7. Argon adsorption−desorption isotherm at 77 K for the wedge pore with the wide end closed.

end closed is identical to that from a partially filled pore with the narrow end closed, which we shall show.

We begin with an explanation of adsorption and desorption in a wedge pore with the wide end closed. The pore can be identified with an ink-bottle pore model having a linear change in pore width along the axial direction rather than a step change in pore width as in the usual ink-bottle model. Therefore, the isotherm for this pore has the same form as that found for the usual ink-bottle pore models.[6,25] To examine the mechanism of adsorption and desorption, we present snapshots in Figure 8 for various points on the isotherm, from which we can identify four zones and three junctions, which are identical to those for the pore with the narrow end closed.

Adsorption begins with the molecular layering on the pore walls and at the closed end, followed by a condensation that is nucleated at the pore mouth and instantly fills zones 1 and 2. Condensation occurs when the liquid embryo (a thin biconcave lens) is formed at the pore mouth; its radius of curvature is so large that condensation has to occur in both zones 1 and 2 such that the radius of curvature at the completion of this condensation satisfies the Kelvin equation. The number of zones through which condensation takes place depends upon the angle of the wedge. A further increase in pressure will see the advance of the meniscus and a gradual change in density through junction $J_{2,3}$, which is then followed by a sharp condensation in zone 3 and then a gradual change in density at junction $J_{3,4}$. At this point, the last zone (zone 4) is a cavity, and adsorbate condenses here at a higher pressure, typical of an ink-bottle pore. Thus, in summary, the adsorption branch has multiple condensation steps, associated with the sharp filling of zones, combined with gradual changes at the junctions, in much the same way as was observed earlier for the pore with the narrow end closed.

For desorption from a completely filled pore, an interface is formed at the pore mouth of zone 1 (Z_1), and as pressure is decreased from F_1 to F_2 (as marked on the isotherm in Figure 7), the density changes only slightly, because of the stretching of the adsorbate in the pore. This happens mainly at the junctions, where the incommensurate packing makes the adsorbate more compressible[26] rather than in the zones (see the snapshot for point F_2 in Figure 8b). When pressure is decreased further from F_2, there is a sharp evaporation from zones 2, 3, and 4 at the cavitation pressure because the size of the narrow end is smaller than the critical value, which demarcates pore blocking from cavitation.[6,25] At F_3, zone 1 behaves like an open-end wedge pore and, therefore, goes through the usual process of evaporation by the recession of the

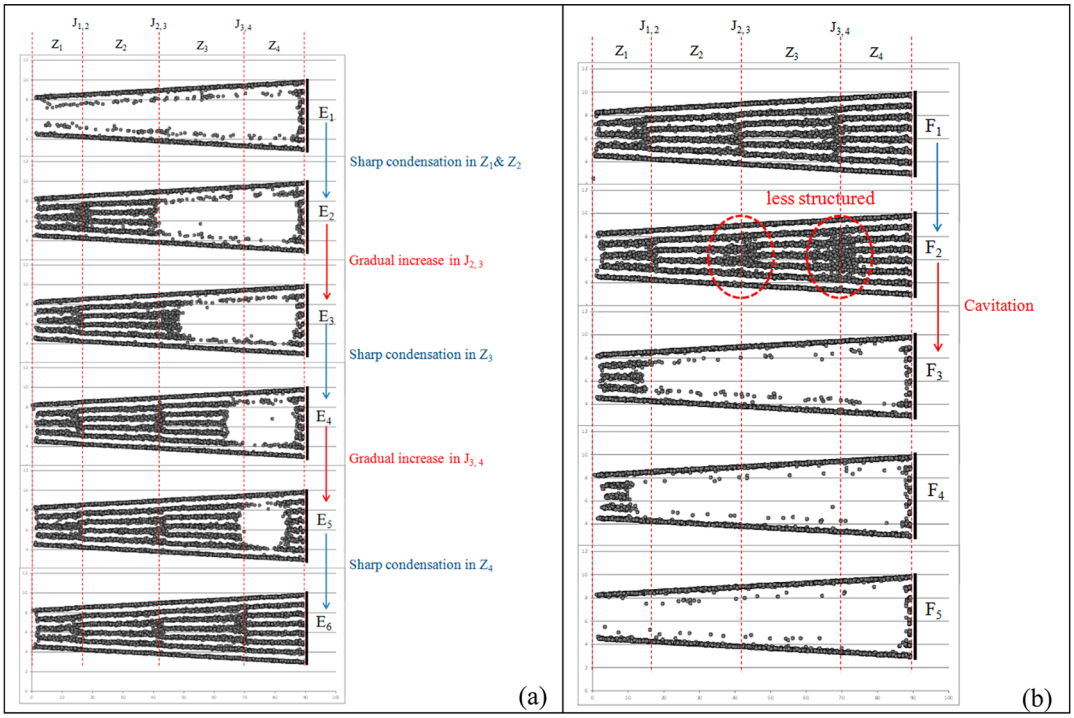

Figure 8. Snapshots for argon adsorption and desorption at 77 K in a wedge pore with its wide end closed: (a) adsorption and (b) desorption. Points E_1−E_6 and F_1−F_5 are marked on the isotherm in Figure 7.

dx.doi.org/10.1021/la5035992 | Langmuir 2014, 30, 12879−12887

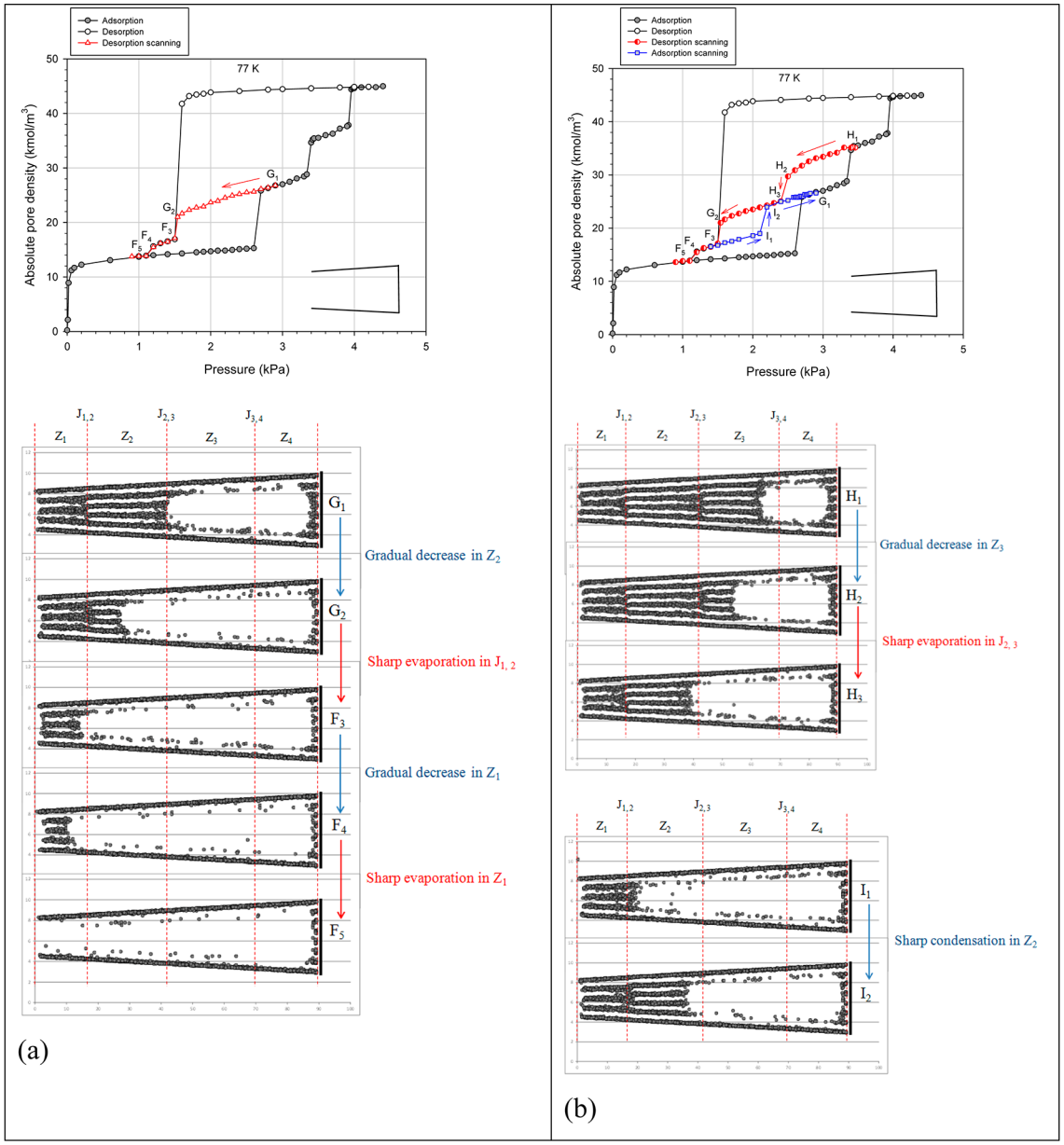

Figure 9. Argon adsorption and desorption in the wedge pore with the wide end closed at 77 K: (a) desorption scanning from points G_1 to F_5 and (b) desorption scanning from points H_1 to F_5 and adsorption scanning from F_3 to G_1.

two menisci to F_4, followed by a sharp evaporation to F_5. This is responsible for the tail observed after the sharp evaporation of zones 2, 3, and 4. Thus, we can conclude that the adsorption and desorption isotherms for the wedge pore with its wide end closed behave in essentially the same way as those of a typical ink-bottle pore.

The scanning curves from various points are shown in Figure 9.

We start with the descending curve from point G_1, where zones 1 and 2 are filled and junction $J_{2,3}$ is partially filled. The adsorbate at this point is identical to that at point A_3 in the pore with its narrow end closed (see Figure 1), and therefore, the descending scanning from point G_1 is the same as the desorption from this pore, i.e., gradual density change in zone 2 to point G_2 and sharp evaporation from junction $J_{1,2}$. We confirm the assertion that the descending scanning curve from a partially filled pore with the wide end closed corresponds to the boundary curve for desorption in the pore with the narrow end closed, by superimposing the isotherms of the two pores in Figure 10.

The same behavior is observed when the descending curve starts from a higher loading at point H_1 in a partially filled pore. The descending scanning is again seen to be essentially the desorption boundary found in the pore with the narrow end closed, i.e., a gradual change in zone 3 (H_1–H_2), followed by a sharp evaporation in junction $J_{2,3}$ to point H_3. This is continued as a gradual change in zone 2 to point G_2 and evaporation from junction $J_{1,2}$. Thus, we see that the descending curves from a partially filled pore (behaving like a pore with the narrow end closed) are within the envelope of the desorption boundary of the completely filled pore. The schematics for the processes just described are summarized in Figure 4b.

Finally, we consider the ascending scanning curve from point F_3, where zone 1 is filled and junction $J_{1,2}$ is partially filled. At this point, the desorption is identical to that already seen in the pore with its narrow end closed; an increase in pressure from

dx.doi.org/10.1021/la5035992 | Langmuir 2014, 30, 12879–12887

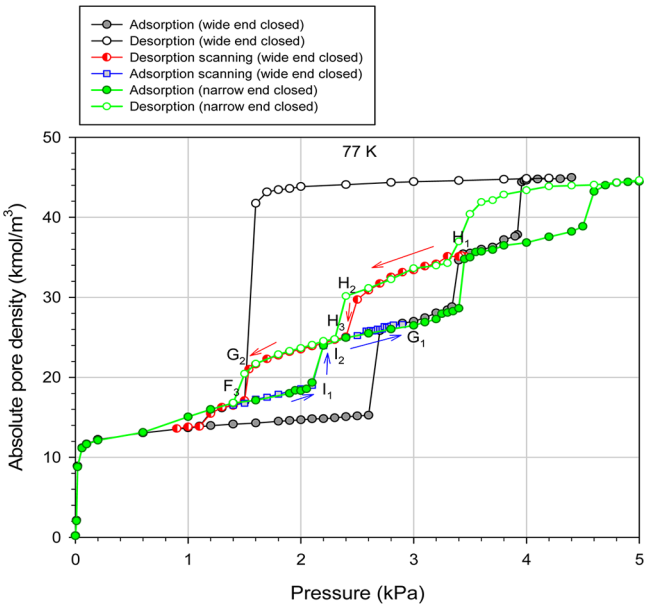

Figure 10. Argon adsorption and desorption in the wedge pores at 77 K.

this point results in a gradual change at junction $J_{1,2}$ up to point I_1, followed by sharp condensation in zone 2 (point I_2). This is continued with the gradual filling of junction $J_{2,3}$, followed by filling of zone 3, etc., until zone 4 is filled by a sharp condensation, as shown in Figures 4a, 9b, and 10.

4. CONCLUSION

We have used GCMC simulation to investigate the hysteresis loop and scanning curve behavior within the hysteresis loop in wedge-shaped pores with either the narrow end or wide end closed.

Hysteresis Loop. Multiple hysteresis loops are observed for wedge pores with either the narrow end or wider end closed. For the wedge pore with the narrow end closed, adsorption and desorption follow a repeated sequence with two stages: rapid change in pore density, followed by a gradual change. These two stages define zones where the packing of the adsorbate is commensurate with the pore width and junctions (between zones) where the adsorbate packing is incommensurate. The most interesting feature is that the sequence of these two stages is opposite for adsorption and desorption. In adsorption, the gradual increase in density is associated with the junction and the sharp condensation is associated with the zone between adjacent junctions. The opposite is found in the desorption process; here, the gradual decrease and sharp evaporation are associated with the zone and junction, respectively. For the wedge pore with its wide end closed, the adsorption branch follows essentially the same path as the pore with its narrow end closed, with the exception that the sharp condensation in zones 1 and 2 occurs simultaneously for the chosen wedge angle studied in this paper. The desorption branch follows the same cavitation behavior as is commonly observed in ink-bottle pores with a step change in the pore width between neck and cavity.

Scanning Curves. For the wedge pore with the narrow end closed, a descending curve traces completely the portion of the adsorption boundary of the isotherm where the density change is gradual and then crosses the hysteresis loop to the desorption boundary to a point having the same adsorbate density. The same is true for the ascending curve. The scanning curve is reversible across the hysteresis loop.

For the wedge pore with the wide end closed, the descending curve from a partially filled pore behaves identically to the desorption branch of the wedge pore with the narrow end closed. The same behavior is found for the ascending curve.

AUTHOR INFORMATION

Corresponding Author

*E-mail: d.d.do@uq.edu.au.

Notes

The authors declare no competing financial interest.

ACKNOWLEDGMENTS

This work is supported by the Australian Research Council. The authors also acknowledge the support from the Thailand Research Fund (Contract TRG5780126) and the Internationalization for Research University (IRU) of Naresuan University.

REFERENCES

(1) Fan, C.; Do, D. D.; Nicholson, D. Condensation and evaporation in capillaries with nonuniform cross sections. *Ind. Eng. Chem. Res.* **2013**, *52*, 14304−14314.

(2) Nguyen, P. T. M.; Do, D. D.; Nicholson, D. Pore connectivity and hysteresis in gas adsorption: A simple three-pore model. *Colloids Surf., A* **2013**, *437*, 56−68.

(3) Reichenbach, C.; Kalies, G.; Enke, D.; Klank, D. Cavitation and pore blocking in nanoporous glasses. *Langmuir* **2011**, *27*, 10699−10704.

(4) Morishige, K. Adsorption hysteresis in ordered mesoporous silicas. *Adsorption* **2008**, *14*, 157−163.

(5) Ravikovitch, P. I.; Neimark, A. V. Experimental confirmation of different mechanisms of evaporation from ink-bottle type pores: Equilibrium, pore blocking, and cavitation. *Langmuir* **2002**, *18*, 9830−9837.

(6) Klomkliang, N.; Do, D. D.; Nicholson, D. Effects of temperature, pore dimensions and adsorbate on the transition from pore blocking to cavitation in an ink-bottle pore. *Chem. Eng. J.* **2014**, *239*, 274−283.

(7) Hitchcock, I.; Lunel, M.; Bakalis, S.; Fletcher, R. S.; Holt, E. M.; Rigby, S. P. Improving sensitivity and accuracy of pore structural characterisation using scanning curves in integrated gas sorption and mercury porosimetry experiments. *J. Colloid Interface Sci.* **2014**, *417*, 88−99.

(8) Cychosz, K. A.; Guo, X.; Fan, W.; Cimino, R.; Gor, G. Y.; Tsapatsis, M.; Neimark, A. V.; Thommes, M. Characterization of the pore structure of three-dimensionally ordered mesoporous carbons using high resolution gas sorption. *Langmuir* **2012**, *28*, 12647−12654.

(9) Rasmussen, C. J.; Vishnyakov, A.; Thommes, M.; Smarsly, B. M.; Kleitz, F.; Neimark, A. V. Cavitation in metastable liquid nitrogen confined to nanoscale pores. *Langmuir* **2010**, *26*, 10147−10157.

(10) Monson, P. A. Understanding adsorption/desorption hysteresis for fluids in mesoporous materials using simple molecular models and classical density functional theory. *Microporous Mesoporous Mater.* **2012**, *160*, 47−66.

(11) Grosman, A.; Ortega, C. Influence of elastic deformation of porous materials in adsorption−desorption process: A thermodynamic approach. *Phys. Rev. B: Condens. Matter Mater. Phys.* **2008**, *78*, 085433.

(12) Cimino, R.; Cychosz, K. A.; Thommes, M.; Neimark, A. V. Experimental and theoretical studies of scanning adsorption−desorption isotherms. *Colloids Surf., A* **2013**, *437*, 76−89.

(13) Esparza, J. M.; Ojeda, M. L.; Campero, A.; Dominguez, A.; Kornhauser, I.; Rojas, F.; Vidales, A. M.; Lopez, R. H.; Zgrablich, G. N_2 sorption scanning behavior of SBA-15 porous substrates. *Colloids Surf., A* **2004**, *241*, 35−45.

(14) Everett, D. H.; Smith, F. W. A general approach to hysteresis. Part 2: Development of the domain theory. *Trans. Faraday Soc.* **1954**, *50*, 187−197.

(15) Coasne, B.; Gubbins, K. E.; Pellenq, R. J.-M. Domain theory for capillary condensation hysteresis. *Phys. Rev. B: Condens. Matter Mater. Phys.* **2005**, *72*, 024304.
(16) Everett, D. H. In *The Solid−Gas Interface*; Flood, E. A., Ed.; Marcel Dekker: New York, 1967; Vol. *2*, pp 1055−1113.
(17) Tompsett, G. A.; Krogh, L.; Griffin, D. W.; Conner, W. C. Hysteresis and scanning behavior of mesoporous molecular sieves. *Langmuir* **2005**, *21*, 8214−8225.
(18) Morishige, K. Hysteresis critical point of nitrogen in porous glass: Occurrence of sample spanning transition in capillary condensation. *Langmuir* **2009**, *25*, 6221−6226.
(19) Broekhoff, J. C. P.; van Beek, W. P. Scanning studies on capillary condensation and evaporation of nitrogen. Part 2. Analysis of ascending and descending scanning curves within B-type hysteresis loops. *J. Chem. Soc., Faraday Trans. 1* **1979**, *75*, 42−55.
(20) Allen, M. P.; Tildesley, T. P. *Computer Simulation of Liquids*; Clarendon: Oxford, U.K., 1987.
(21) Bojan, M. J.; Steele, W. A. Computer simulation of physisorption on a heterogeneous surface. *Surf. Sci.* **1988**, *199*, L395−L402.
(22) Bojan, M. J.; Steele, W. A. Computer simulation of physisorption krypton on a heterogeneous surface. *Langmuir* **1989**, *5*, 625−633.
(23) Bojan, M. J.; Steele, W. A. Computer simulation of physical adsorption on stepped surfaces. *Langmuir* **1993**, *9*, 2569−2575.
(24) Nickmand, Z.; Do, D. D.; Nicholson, D.; Aghamiri, S. F.; Khozanie, M. R. T.; Sabzyan, H. GCMC simulation of argon adsorption in wedge shaped mesopores of finite length. *Adsorption* **2013**, *19*, 1245−1252.
(25) Klomkliang, N.; Do, D. D.; Nicholson, D. On the hysteresis loop and equilibrium transition in slit-shaped ink-bottle pores. *Adsorption* **2013**, 1−18.
(26) Razak, M. A.; Nguyen, V. T.; Herrera, L. F.; Do, D. D.; Nicholson, D. Microscopic analysis of adsorption in slit-like pores: Layer fluctuations of particle number, layer isosteric heat and histogram of particle number. *Mol. Simul.* **2011**, *37*, 1031−1043.